Chapter 1

Recent Trends in Electrospinning of Polymer Nanofibers and their Applications as Templates for Metal Oxide Nanofibers Preparation

Moustafa M. Zagho and Ahmed Elzatahry

Additional information is available at the end of the chapter

http://dx.doi.org/10.5772/65900

Abstract

Scientists have been paying a special attention for the synthesis of one-dimensional (1D) morphologies to attain new phenomena and novel physicochemical characteristics of materials. Furthermore, 1D nanostructures exhibit long axial ratio, which has a great influence on the physical and chemical properties of materials. It is worth mentioning that electrospinning is one of the most common and efficient techniques used for the preparation of 1D polymer composite nanofibers. Using electrospinning, nanofibers were fabricated by electrostatic stretching of polymer viscous solution by applying a high voltage. This chapter discusses the synthesis of metal oxide nanofibers such as tin oxide (SnO_2), zinc oxide (ZnO), titanium oxide (TiO_2), and nickel oxide (NiO) using electrospinning process of polymer solution containing metal precursors and followed by annealing procedures to eliminate the polymer galleries, which were chosen as a sacrificial template for the preparation of metal oxide nanofibers. SEM, XRD, and XPS are equipped to characterize the electrospun metal oxide nanofibers and the results settle the formation of homogeneously distributed metal oxide nanofibers.

Keywords: electrospinning, metal oxide, nanofibers, SEM, XRD, XPS

1. Introduction

In the last decades, electrospinning attracted a vast portion of attention from both research and commercial points of view. Scientists paid great interest for electrospinning because of its ability to yield fibers in the submicron scale that are very hard to attain by handling standard mechanical fiber-spinning procedures [1–5]. Electrospinning is a technology that is

broadly applied to fabricate polymer fibers with diameters ranging from 2 nm to several micrometers and is also known to have unique properties such as high surface area, controlled porosity, and mechanical strength [6–9]. The pore structure and the diameters of the produced fabrics and nanofibers can be controlled using this technique [10, 11]. Electrospun fibers have been successfully used in varied applications including protective clothing, biomedical, pharmaceutical, security, environmental engineering, chemical sensors, and electrode materials [12–19].

Recently, electrospinning has been used in the research of natural and synthetic polymer nanofibers [20] such as cellulose [21], polyurethanes [22], collagen [23] and hyaluronic acid [24]. Electrospinning can be handled to obtain large quantities of fibers using two-layer electrospinning scheme. This technique consists of a lower layer, which contains a ferromagnetic suspension, and an upper layer, which contains the polymer solution, and the multiple nozzles are arranged in lines or circles. One such example is the bubble electrospinning, which is demonstrated and developed by many researchers [25, 26]. Dosunmu et al. reached high production rates of fibers by using porous hollow tube to obtain multiple jets and by increasing the tube length and the number of holes [27]. In addition, coelectrospinning of different polymers has been reported to control the morphology and tailor the voids volume [28–30].

1.1. Electrospinning process

Electrospinning setup consists of a high voltage power supply, spinneret (like pipette tip), and grounded collected plates (like metal screen) and is conducted at room temperature. Polymer solution is charged by applying high voltage and then accelerated toward the collector, which is of opposite polarity [31, 32]. The polymer must be dissolved first before using in electro-

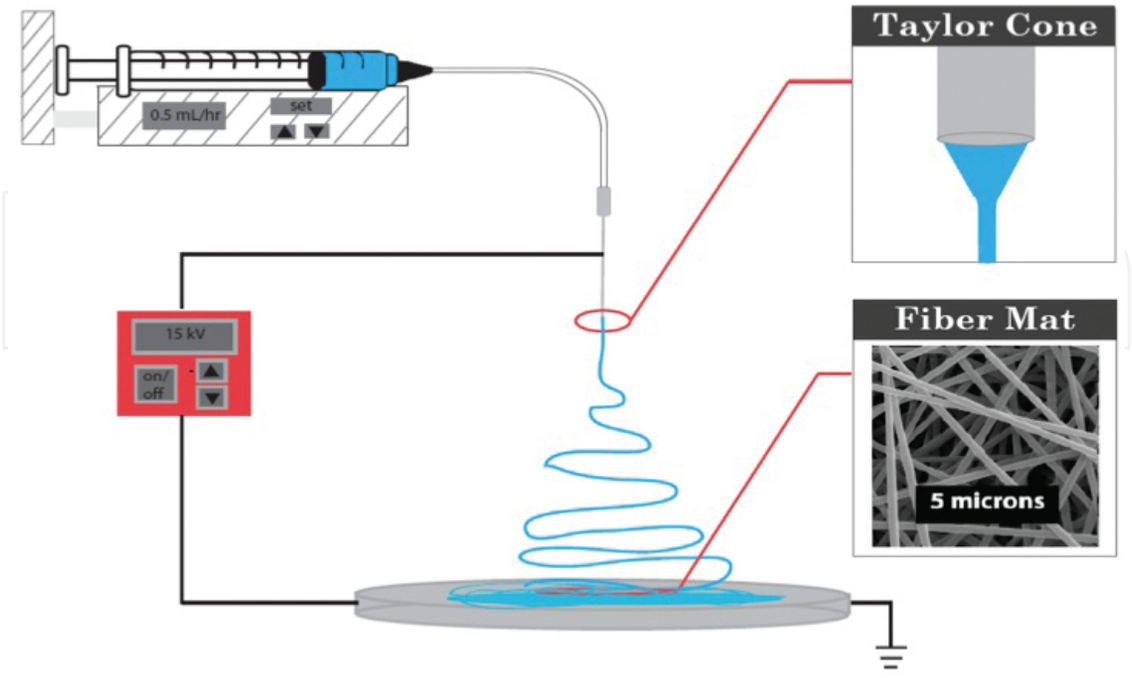

Figure 1. Schematic diagram of vertical electrospinning apparatus.

http://dx.doi.org/10.5772/65900

spinning and then introduced into the capillary tube. At critical voltage, the electrostatic forces counteract the surface tension of the used polymer solution and an electrified jet is produced and ejected from the tip of the Tylor cone and then the solvent will be evaporated and leaving a polymer nanofiber [33, 34]. Currently, there are two standard sets of electrospinning: vertical and horizontal. The vertical electrospinning is represented in **Figure 1**.

The diameters and morphology of electrospun nanofibers are measured by numerous parameters, which are classified into solution, process, and ambient parameters. These factors are demonstrated clearly in **Figure 2**.

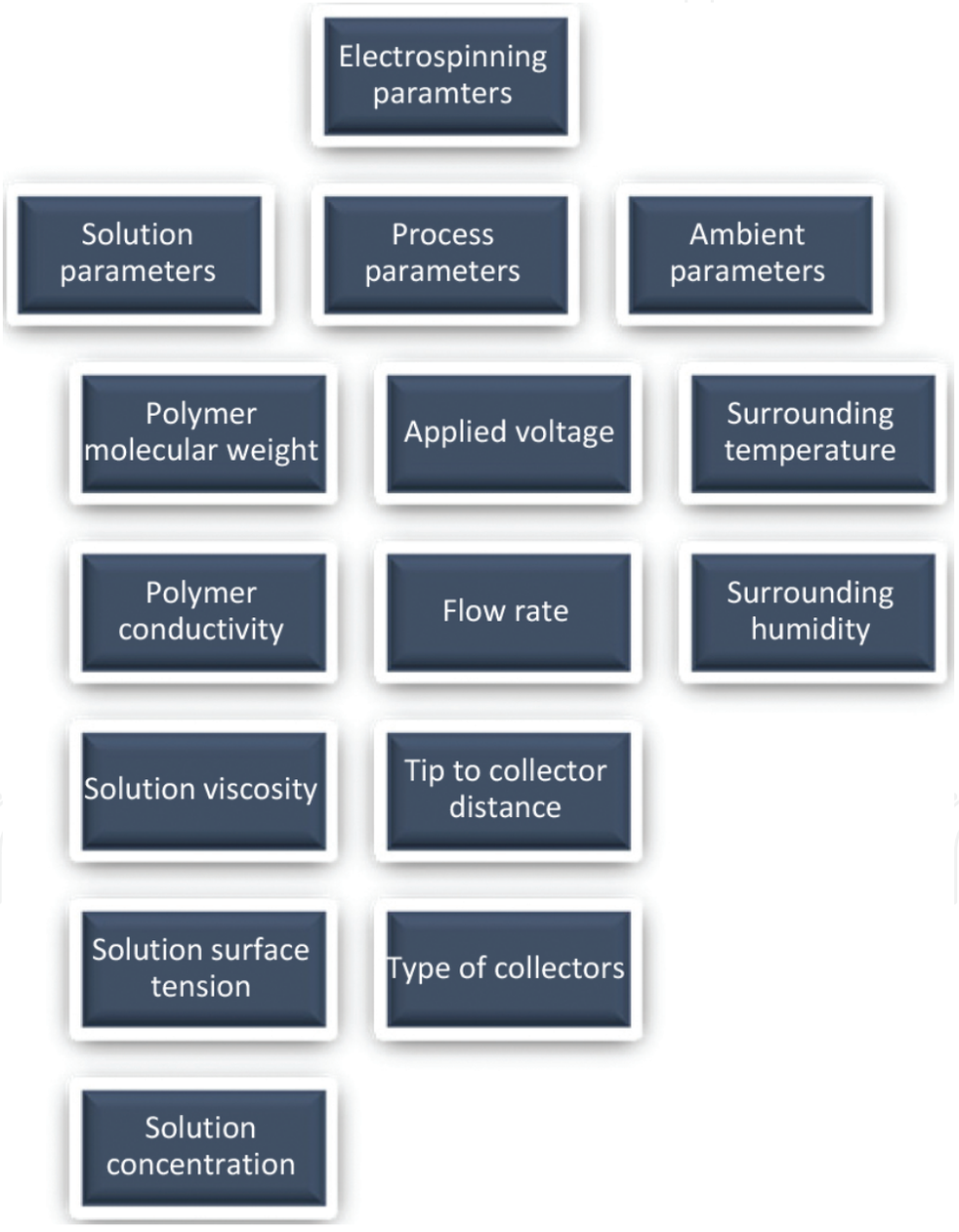

Figure 2. Factors affecting on elctrospinning technique.

2. Polymers favored in electrospinning technique

More than 200 polymers (natural, synthetic, and copolymers) were used in electrospinning successfully depending on their applications [35].

2.1. Natural polymers

Nowadays, polymer nanofibers are used in a wide variety of applications in various industries and also in other arenas. Natural polymers are preferred over synthetic polymers in medical and biological uses because of their low immunogenicity and better biocompatibility. Recent researchers have reported the use of electrospinning process of natural polymers such as gelatine, collagen, and silk fibroin [36–41]. It was mentioned that some natural polymers such as collagen lose their properties after electrospinning using fluoro alcohols [42]. To resolve this problem, highly volatile fluoro alcohol such as 2,2,2-trifluoroethanol is used during electrospinning of collagen [43]. Yang et al. [44] found that about 45% of collagen is lost during electrospinning process. In addition, beads formation represents another challenge for the preparation of natural polymer nanofibers. For instance, laminin I nanofibers are fabricated with beads in the mesh structure and this may be related to the presence of the cross-linking agent and these results are reported by Neal et al. [45].

2.2. Synthetic polymers

Synthetic polymers are favored over natural polymers in certain uses because synthetic polymers can be tailored to develop the mechanical and degradation properties [46]. Certain synthetic polymers can be used in biomedical applications with some limitations including polylactide (PLA) [47] and polyglycolide (PGA) [48] to produce electrospun nanofibrous scaffolds.

2.3. Copolymers

Copolymers appear as an attractive opportunity to obtain new structures with desirable characteristics from electrospinning and also have better efficiency than that of homopolymers. The mechanical, thermal, morphological, and biodegradability properties of polymers can be tailored by using copolymers in electrospinning process. Incorporation of the hydrophilic polymer of hydrophobic polyesters enhanced the cell affinity of this sort of polyesters. Moreover, the stiffness of poly (ethylene-co-vinyl alcohol) (PEVA) is improved after the addition of poly (glycolide) (PGA) [49]. Also, copolymerization of methyl methacrylate (MMA) with methacrylic acid (MAA) improved the thermal stability of poly methyl methacrylate [50]. In addition to that, electrospun scaffolds produced from poly (p-dioxanone-co-L-lactide)-block-poly (ethylene glycol) (PPDO/PLLA-B-PEG) have enhanced hydrophilicity and biodegradability due to the addition of PEG to PPDA-PLLA blends [51].

http://dx.doi.org/10.5772/65900

3. Metal oxide nanofibers

Metal oxide materials are critically important from both the academic and industrial point of views. Scientists have been paying a special attention for the synthesis of one-dimensional (1D) morphologies to attain new phenomena and novel physicochemical characteristics of materials.

3.1. Synthesis of crystalline metal oxide nanofibers and their applications

It is worth mentioning that electrospinning is the most common technique used for the preparation of 1D polymer composite nanofibers [52, 43]. Furthermore, 1D nanostructures exhibit long axial ratio, which has a great influence on the physical and chemical properties of materials. Using electrospinning, nanofibers are fabricated by electrostatic stretching of a viscous solution of polymer composites by applying a high voltage [3]. In the recent years, scientists have focused on the fabrication of metal oxide nanofibers such as tin oxide (SnO_2), zinc oxide (ZnO), titanium oxide (TiO_2), and nickel oxide (NiO) through the electrospinning of polymer solution containing metal precursors and followed by annealing procedures [53–57]. Depending on the thermal degradation of polymers, certain polymers such as polyvinyl alcohol (PVA) and polyacrylonitrile are chosen as a sacrificial template for the fabrication of metal oxide nanofibers. After the annealing process, the organic components will be degraded and the metals will be oxidized by inorganic precursors giving nanofibers the desired metal oxide.

3.1.1. Tin oxide (SnO_2) nanofibers

Recently, high interest has been paid to one-dimensional tin oxide (SnO_2) nanostructures. There are various techniques designed for the synthesis of different structures of SnO_2, such as electrospinning, self-catalytic, thermal evaporation, and thermal oxidation techniques [58–62]. The metal oxide fibers are commonly employed in gas detection application. The gas-sensitive characteristics of the prepared sensors are due to its high conductivity alterations when the prepared sensors adsorb or desorb a very low loading of chemical compounds on its surface [63–72]. High adsorption-desorption gas sensors in one-dimensional nanostructures were developed using metal oxide nanofibers owing to its highly porous networks [73, 74]. The morphological nature of the upper surface layer usually controls the molecular adsorption-desorption process, the response, and the sensitivity of the sensors. Metal oxide nanofibers are employed as a sensitive sheet instead of a thin film deposited by conventional processes such as drop, spinning, and airbrush because of its large surface area and, consequently, a thin film of metal oxide nanofibers enhances the sensitivity and the speed of the reaction.

Santos et al. [75] prepared SnO_2 nanofibers by electrospinning process of PVA/$SnCl_4.5H_2O$ composite followed by annealing at 450°C to eliminate PVA matrix. The fabricated SnO_2 electrospun nanofibers are designed as sensitive layers for resistive chemical sensors. The produced fibers exhibit high sensitivity, reproducibility, and quick reaction in the recognition of triacetone triperoxide (TATP) explosive precursors in the ppm scale. In addition, SnO_2 hollow nanofibers were fabricated for a high and fast detecting ethanol (C_2H_5OH) using

polyvinylpyrrolidone (PVP) as a template, which was removed by calcination at 600°C for 2 h [76]. The produced SnO_2 nanofibers have a large surface area of 26.43 m^2g^{-1} and grain sizes of about 20 nm. Another study by Choi et al. [77] concerns the preparation of Pd-doped SnO_2 hollow nanofibers for methane (CH_4), H_2, carbon monoxide (CO), and C_2H_5OH detection. They studied the effect of temperature and Pd-doping content on the detection for CH_4, H_2, CO, and C_2H_5OH. They noticed a dramatic variance in the selectivity for these compounds between undoped and Pd-doped SnO_2 hollow nanofibers. The selective detection of C_2H_5OH was tested with undoped and 0.08 wt% Pd-doped SnO_2 hollow nanofibers. The study showed a significant decline in C_2H_5OH detection in case of using 0.4 wt% Pd when the temperature is raised from 330 to 440°C, while the responses to CH_4 and H_2 were improved and, consequently, they adjusted the selectivity of CH_4 and H_2 at 440°C with minimum interloping to C_2H_5OH. It was worth studying the enhancement of Pr-doping on the gas sensing performance due to its effective influence on the electronic and structural characteristics of materials. Li et al. [78] discussed the fabrication of Pr-doped SnO_2 hollow nanofibers for ethanol detection. They subjected a solution of PVP, $SnCl_2.2H_2O$, and $Pr(NO)_3.6H_2O$ for electrospinning. The prepared nanofibers sample was then annealed at 600°C for 2 h. It was reported that 0.6 wt% Pr-doped SnO_2 nanofibers gave the highest sensitivity and response for ethanol at 300°C. This may be related to the high surface area of the porous morphology and the increment in oxygen vacancy leading to enhanced oxygen absorption. Furthermore, Du et al. [79] focused on the fabrication of In_2O_3/SnO_2 nanofibers for formaldehyde gas sensors using bipolar electrospinning setup of double jets with opposite electric fields. Different sensors composition based on SnO_2, In_2O_3, and In_2O_3/SnO_2 nanofibers were tested at 375°C with 0.5–50 ppm of formaldehyde gas. The formaldehyde selectivity of In_2O_3/SnO_2 nanofibers is higher than that of SnO_2 and In_2O_3 nanofibers. The selectivity values for 0.5 and 50 ppm of formaldehyde were 2.2 and 18.9, respectively. In_2O_3/SnO_2 nanofibers have a good detection of formaldehyde in the interfere gasses of methanol, ethanol, acetone, and ammonia. In addition, Tang et al. [80] synthesized hollow hierarchical ZnO/SnO_2 nanofibers composite for methanol sensing applications. A solution of PVP, $SnCl_2.2H_2O$, and $Zn(NO_3)_2.6H_2O$ is used to prepare electrospun fibers, and then subjected to annealing at 600°C for 3h. This study noted that the nanofibers of ZnO/SnO_2 with a molar ratio of 1:1 exhibited an interesting methanol detection response at 350°C in the presence of interfering gasses.

3.1.2. Zinc oxide (ZnO) nanofibers

Another metal oxide of recent interest is ZnO, which is a chemically stable, nontoxic and inexpensive compound that exhibits high binding energy of 60 mV at 30°C and a direct band gap of 3.37 eV [81]. ZnO is industrially applied in a wide range of uses including chemical sensors, ultraviolet light-emitting diodes, dye-sensitized solar cells, functional instruments, piezoelectric materials, and transparent conductors [82–85]. The morphology, crystal structure, quality, and dimensions of ZnO control its electronic characteristics for different applications [86, 87].

The effective structures of 1D ZnO nanofibers have a small quantum restriction of charge carriers and this measure the performance of nanoscale devices [88–91]. Recent articles

reported the synthesis of ZnO or ZnO-based nanofibers. Ding et al. [92] addressed the unique characteristics of ZnO nanofibers such as high hydrophobicity, development of nanograins, and electrical properties. The study reported the synthesis of super-hydrophobic ZnO nanofibers through a simple combination of wet chemical and electrospinning techniques. The produced ZnO nanofibers have been coated by fluoroalkyl silane (FAS) to obtain super-hydrophobic ZnO nanofibers. Because of the FAS modification, the fibrous ZnO films were transformed from super-hydrophilic (water contact angle (WCA) of 0°) to super-hydrophobic (WCA of 165°). Electrospinning technique was designed to produce nanofibers with a smooth surface which limits its use in some applications as the cohesion forces will be feeble, and thus rough surface nanofibers are preferred. In this context, Barakat et al. [93] mentioned that the electrospinning of colloidal solutions is useful for synthesizing rough surface ZnO nanofibers. The fibers were produced by electrospinning a colloidal solution of PVA, zinc nanoparticles (ZnNPs), and zinc acetate dehydrate (ZnAc) and then followed by calcination. Furthermore, Zhang et al. [94] addressed the fabrication of a hollow ZnO nanofibers using a ZnNPs-free solution. The study reported the preparation of ZnO hollow nanofibers with diameters of 120–150 nm using an electrospinnable solution of PAN, PVP, and ZnAc composites, then followed by calcination to remove the used polymers. They obtained core-shell structure from elctrospinning process where PAN was the core and PVP/ZnAc composite was the shell. ZnO hollow nanofibers showed interesting results related to sensing characteristics against C_2H_5OH. Another study by Kanjwal et al. [95] reported the preparation of rough ZnO hierarchical nanofibers as a photocatalyst against methylene blue dehydrate. They electrospun a colloidal solution consisting of ZnNPs, PVA, and ZnAc dehydrate and then followed by a calcination step at 500°C. Moreover, electrospinning a mixture of high molecular weight PVP and ZnAc in dimethylformamide (DMF) synthesized 1D polycrystalline ZnO nanofibers with porous morphologies [96]. The study reported the effect of ZnAc loadings from 10 to 15 wt% after calcination process from 350 to 650°C onto the produced nanofibers. The prepared ZnO nanofibers were utilized for water treatment as a result of its photocatalytic performance.

A comparative study to compare the undoped and Ce-doped ZnO hollow nanofibers for acetone detection was carried by Li et al. [97]. The used electrospinning solution consisted of cerium nitrate, ZnAc, and PVP. The sample was then followed by calcination at 600°C for 1.5 h. The study declared that Ce-doped ZnO nanofibers are very sensitive to acetone at 260°C. This is ascribed to the morphological and electronic modification in the presence of Ce-doping. Moreover, Al-Ga co-doped ZnO nanofibers have attracted high interest because of its excellent cost effectiveness, conductivity improvement, and mechanical flexibility enhancement. Park and Han [98] reported the preparation and the characterization of Al-Ga co-doped ZnO nanofibers by electrospinning a solution of zinc acetate dihydrate, aluminum nitrate nonahydrate, gallium nitrate hydrate, and PVA and then by annealing at 550°C. The study showed a variation of the lattice parameter with the addition of Ga beyond 2 at.% Al-doping owing to smaller gaps in the atomic size. Consequently, more Ga content can be added without extensive strain. Al-Ga co-doped ZnO nanofibers with 2 at.% Al and 1 at.% Ga exhibit the highest conductivity of 9.57 $\times 10^{-3}$ Scm^{-1}. In addition, Ga incorporation to 2 at.% Al-ZnO nanofibers developed the mobility and the degree of crystallinity.

3.1.3. Titanium oxide (TiO_2) nanofibers

Wu et al. [99] addressed the usage of TiO_2 in many applications including solar, optoelectronic, and catalytic devices. TiO_2 exists in different morphologies such as rutile, anatases, brookite, TiO_2 B (bronze), and TiO_2 R (ramsdellite). It is worth mentioning that the most chosen TiO_2 crystal phase for lithium ion batteries is the anatase structure due to its high capacity and low-cost production [100–102].

He et al. [103] reported the fabrication of 100–300 nm conductive TiO_2 nanofibers using KOH treatment. In this study, a mixture solution of PVP and titanium tetraisopropanolate was used to produce nanofibers for supercapacitor electrode applications using electrospinning. The as-prepared nanofibers exhibit high conductivity, high cycling stability, and high surface area with a stable specific capacitance even after 10,000 cycles and it is enhanced from 0.02 Fg^{-1} to 28.94 Fg^{-1} at 50 mVs^{-1}.

Another study discussed the influence of Ag incorporation to TiO_2 nanofibers on H_2S detecting characteristics. Pristine and Ag nanoparticles/TiO_2 (Ag/TiO_2) nanofibers were fabricated by Ma et al. [104]. H_2S sensing measurements showed that Ag/TiO_2 nanofibers have much higher detection responses and sensitivity than that of pristine Ag/TiO_2 nanofibers. It is found that the implementation of AgNPs leads to phase conversion of TiO_2 to rutile from anatase phase.

For the catalytic performance of TiO_2 nanofibers, Hao et al. [105] reported that mesoporous Au/TiO_2 nanofibers were obtained by incorporating Au nanoparticles (AuNPs) to TiO_2 nanofibers. The nanofibers were prepared via electrospinning a mixture solution of $Ti(OC_4H_9)_4$, $HAuCl_4$, and PVP. The effect of AuNPs loading (2, 5, and 10 wt%) toward the reduction of 4-nitrophenol (4-NP) to 4-aminophenol (4-AP) by sodium borohydride was reported. The results reported a decrease in the TOF value of the catalyst and an increase in the reaction rate constant with increasing AuNPs loading and this decline may be attributed to the small size and high surface area in case of 2 wt%, AuNPs. In addition, Tolba et al. [106] discussed the synthesis of ZnO nanobranches attaching TiO_2 nanofibers as nonprecious electrocatalyst for ethanol oxidation. The study reported the use of a colloidal solution of titanium isopropoxide, poly (vinyl acetate), and ZnNPs to produce electrospun fibers. Produced nanofibers went through a calcination and hydrothermal treatment. The study concluded that the concentration of ZnNPs has a distinct impact on the electrical conductivity and the electrocatalytic performance of the final nanofibers. For instance, utilizing 0.1 g ZnNPs in the electrospinnable solution produce active and stable nanofibers for ethanol oxidation in alkaline medium. In addition, Li et al. [107] measured the photocatalytic H_2-production activity in water splitting of 1D mesoporous NiO/TiO_2 composite nanofibers. The composite nanofibers were fabricated by electrospinning process of colloidal solution of tetra-n-butyl titanate (TBT), PVP, and $Ni(NO_3)_2.6H_2O$, and then the samples were calcined in air at 500°C for 3 h. It was reported that the H_2-production activity of TiO_2 nanofibers was developed at low NiO content (0–0.5 wt%). In fact, at 0.25 wt% of NiO, the mesoporous composite nanofibers exhibit the highest H_2-production activity. This can be related to the behavior of NiO as an active cocatalyst, which hinders the recombination of photogenerated charge carriers and diminishes the overpotential of H_2 production.

In another research for solar cells, Zr is doped into TiO_2 nanofibers to be utilized as photoanodes of dye-sensitized solar cells (DSCs) [108]. A solution of PVAc, titanium isopropoxy, and zirconium n-propoxy was used to produce nanocomposite electrospun fibers. It was mentioned that the conversion efficiency of DSCs improved after Zr addition. The group tested the effect of Zr-doping amount (0.5, 1,1.5, and 2%) on TiO_2 nanofibers formulations for DSCs. The study reported that the photovoltaic efficiency reached 4.51% in case of 1% Zr-doping, while the efficiency was achieved to 1.61% for cells based on pristine TiO_2 nanofibers. This improvement can be attributed to the electrons transfer and dye loading. In more details, the presence of Zr developed the band gap through decreasing the charge recombination rate and, consequently, increases the electrons transfer (3.217 eV for 1% Zr-doped TiO_2 nanofibers and 3.202 eV for pristine TiO_2 nanofibers). Moreover, the dye loading of pristine TiO_2 nanofibers is found to be 0.52 $\times 10^{-7}$ molcm^{-2}, which is much lower than that of 1% Zr-doped TiO_2 (1.36 $\times 10^{-7}$ molcm^{-2}).

3.1.4. Nickel oxide (NiO) nanofibers

NiO nanofibers exhibit good chemical and thermal stability properties and can be prepared easily using electrospinning. High interest in preparing 3D nickel oxide (NiO) nanofibers technology to be applied in photovoltaic devices has been reported. This is because 3D NiO surfaces exhibit high degree of porosity, which increases the mobility of charge carriers and consequently enhances the efficiency of photovoltaic procedures [109]. Moreover, NiO has been used in batteries and chemical sensors industry because of its attractive characteristics and morphological properties [110, 111].

Macdonald et al. [112] prepared NiO nanofibers for cathode fabrication using electrospinning process of PAN and $Ni(AcAc)_2$. NiO nanofibers were deposited into fluorine-doped tin oxide (FTO) to produce p-type nano photocathodes with a surface area of 0.8 cm^2. To remove all organic residues, the electrode was sintered for 30 min at 450°C. The NiO nanofibers diameters were decreased to approximately 100 nm due to the calcination influence at 500°C and the nanofibers became more rough and straw-like structure owing to the elimination of PAN chains. Furthermore, Jian et al. [113] discussed the electrochemical performance of La-doped NiO nanofibers as positive electrode structures. La-doped NiO nanofibers are produced by the calcination procedure at 650°C for 3 h of electrospinning solution of $Ni(CH_3COO)_2.4H_2O$, $La(NO_3)_3.6H_2O$ and PVA. They designed asymmetric supercapacitor consisting of porous-activated carbon as a negative electrode, as-prepared La-doped nanofibers as a positive electrode, and 2M KOH aqueous solution as an electrolyte. It was seen that the perfect La/Ni loading ratio in the positive electrode was 1.5%. In addition, La-doping was found to develop the specific capacitance and the electrochemical stability. In more details, the specific capacitance became 94.85 F g^{-1}, which is 5.3 times better than the capacitors with undoped NiO nanofibers. Also, the coulomb efficiency of more than 90% is retained even after 1000 cycles.

NiO nanofibers exhibit excellent catalytic behavior. Elzatahry [114] described the use of PAN as a sacrificial template in the electrospinning method to fabricate NiO nanofibers to be designed as an electrocatalyst in methanol oxidation process in alkaline medium. The study reported the use of a solution of PAN and 50 wt% NiO to produce electrospun fibers. Uniform

fibers with a diameter of 145–170 nm and low content of submicron and random nanofibers were produced. Porous NiO nanofibers are obtained after the elimination of PAN at 400°C for 3.5 h.

For sensing applications, Choi et al. [115] studied the fabrication of p-type NiO nanofibers and its activity for CO and NO_2 detection as a function of the size of the nanograins. The electrospinning solution consisted of 8.3 wt% PVA and 4 wt% nickel II acetate tetrahydrate. The produced nanofibers were subjected to calcination at 400–850°C to adjust the nanograins size. It was found that nanograins' size has a limited impact on the CO and NO_2 detection in case of p-type NiO nanofibers. On the other hand, the responses of n-type NiO nanofibers were highly dependent on the nanograins' size. Furthermore, Luo et al. [116] addressed the synthesis of Li-doped NiO nanofibers for nonenzymatic glucose sensing. The group reported the use of solution mixture of PVP, $Ni(NO_3)_2.6H_2O$, and $LiNO_3$ and another solution without $LiNO_3$, then calcined the product at 500°C for 3 h. It was noticed that the average diameter of the formed Li-doped NiO nanofibers was 200 nm, while that of NiO nanofibers was 150 nm. The fabricated Li-doped NiO nanofibers exhibit high surface area, high conductivity, and high electrocatalytic performance through holes and defective sites, which develop the electrons transfer process. In addition, SnO_2/NiO composite nanofibers were used in humidity sensing applications [117]. The study reported the use of electrospinning solution of $SnCl_2.2H_2O$, $NiCl_2.6H_2O$, and PVP and then annealed the produced fibers at 600°C for 3 h. It was noted that the high sensitivity of SnO_2/NiO nanofibers to humidity is ascribed to the active surface area that increases the conduction in the presence of water vapor.

3.2. Morphological characterization of metal oxide nanofibers

Morphological measurements of metal oxide nanofibers including fibers orientation, fibers distribution, and fibers diameters can be measured using many analytical instruments such as scanning electron microscope (SEM), X-ray diffraction (XRD), and X-ray photoelectron spectroscopy (XPS).

3.2.1. Scanning electron microscope characterization (SEM)

Scanning electron microscope (SEM), field emission scanning electron microscope (FESEM), transmission electron microscope (TEM), polarized light microscope, and atomic force microscope (AFM) can be utilized to study the nanofibers' diameters. It is worth mentioning that the high-resolution capability offered by SEM makes it a conventional technique to analyze nanofibers of which their structures are measured by their functionalities. The SEM is also used to study the chemical composition and surface topology and morphology. The nanograph's resolution is controlled by the interaction between the electron probes with metal oxide nanofibers. In more details, SEM measurements require conductive polymers and a small sample for morphology study. SEM analysis is a quick method used to measure the fiber diameters using a gold coating.

Figure 3 represents the SEM micrograph of electrospun ZnO nanofibers fabricated by Kanjwal et al. [95]. **Figures 3(A)** and **(B)** confirms the formation of continuous and smooth nanofibers

http://dx.doi.org/10.5772/65900

of ZnAc/PVA. Furthermore, the addition of Zn NPs did not affect the structure of the produced nanofibers without any beads formation as clearly represented in **Figures 3(C)** and **(D)**. It should be also mentioned that the average diameters of the fabricated nanofibers are decreased after calcination process at 500°C for 90 min and this significant decrease can be attributed to the elimination of polymer matrix due to calcination at high temperatures. The shape of the nanofibers is not influenced by the addition of Zn NPs in general but there is an influence on the nanofibers' surface. Moreover, the surface of the nanofibers was relatively smooth in the case of Zn/Ac, while the addition of Zn NPs produced nanofibers with a rough surface.

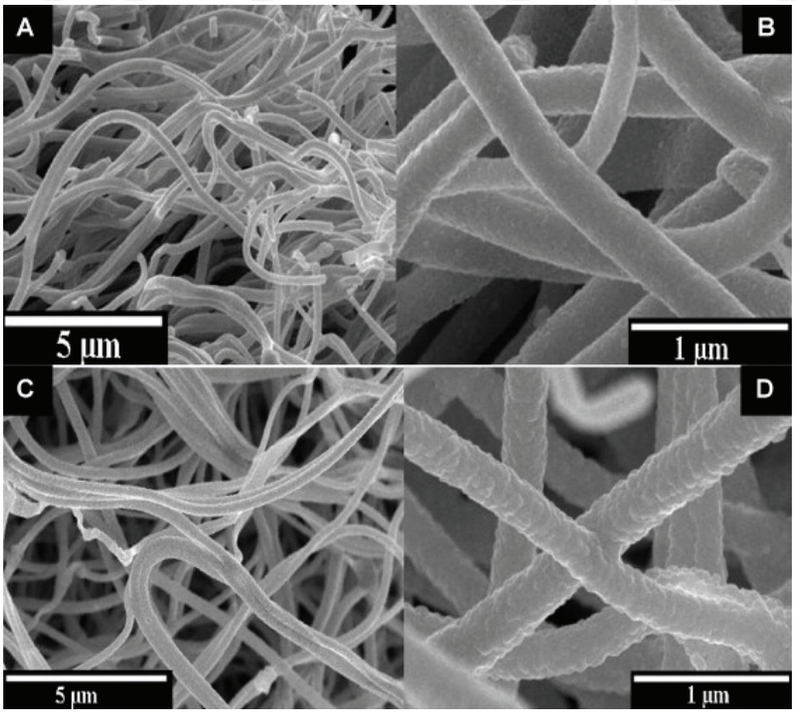

Figure 3. Low and high magnification SEM images of the powder obtained after calcination of ZnAc/PVA nanofibers mats (A and B), and Zn NPs/ZnAc/PVA (C and D) at 500°C for 90 min [95].

3.2.2. X-ray diffraction (XRD) characterization

XRD analysis is handled to study the crystal morphologies of various solids and metal fibers, including the lattice constants and geometry, the orientation of the single crystal, crystallite size, and crystal defects. The degree of crystallinity of the produced metal oxide nanofibers can be calculated from X-ray diffraction (XRD), both wide angle and small angle (WAXS and SAXS) and also from differential scanning calorimetry (DSC). A solid sample of metal oxide nanofibers is irradiated with X-rays of fixed wavelength while the angle of the diffracted X-ray beam is controlled as a function of the intensity of the diffracted beam. Moreover, each lattice plane satisfies Bragg's equation from which the values of the d-spacing between platelet sheets can be determined. XRD analysis was achieved to measure the crystal structures of the calcined ZnO nanofibers prepared by Kanjwal et al. [95] as described in **Figure 4**.

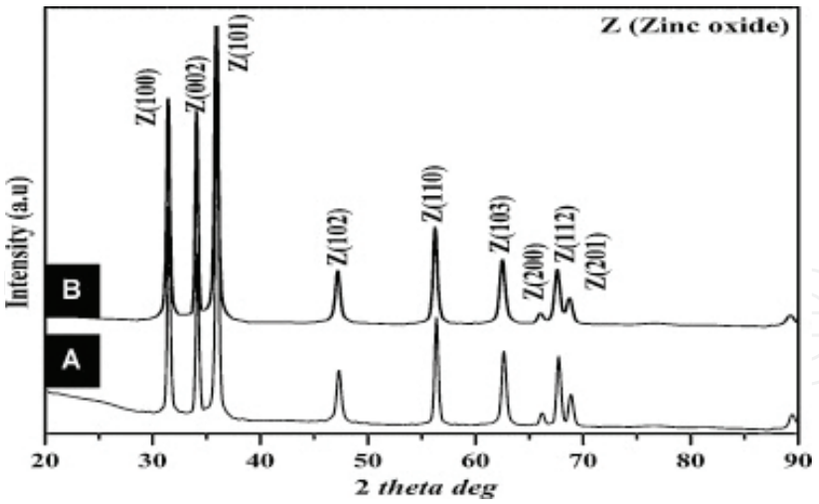

Figure 4. XRD patterns of nanofibers after calcination of (A) Zn NPs-free and (B) the hydrothermal product [95].

XRD results, in this case, confirm the synthesis of ZnO nanofibers. A SPECTRUM A of the annealed ZnO nanofibers confirms the formation of pure ZnO powder. It should be also noticed that the XRD spectra are not influenced by the incorporation of Zn NPs. In addition, the hydrothermal product has the same beaks as represented in spectra B.

3.2.3. X-ray photoelectron spectroscopy (XPS)

Another important characterization tool to investigate the surface chemistry of electrospun metal oxide nanofibers is X-ray photoelectron spectroscopy (XPS). The surface chemical nature

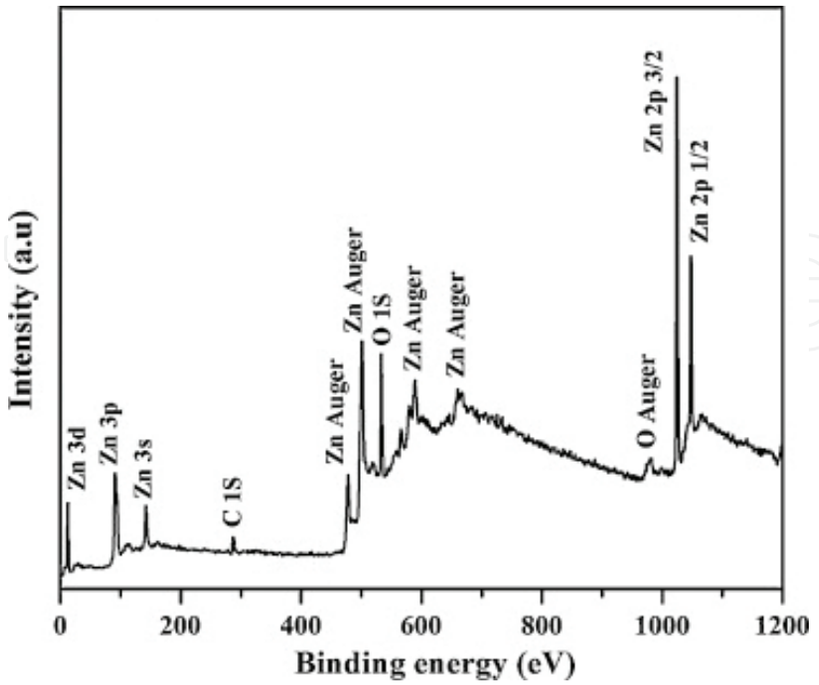

Figure 5. XPS data of the hydrothermally fabricated ZnO nanofibers [95].

of the metal oxide nanofibers can be estimated by its hydrophilicity which can be characterized by using XPS. XPS is performed to support the obtained XRD results and to measure the oxidation states and the changes in binding energies. The possible changes in binding energies of the prepared ZnO nanofibers have been reported by Kanjwal et al. [95] as represented in **Figure 5**. The peak of C 1s at 284 eV is related to the graphite tape employed in the sampling. The Zn 2p region in ZnO sample consists of the main 2p3/2 and 2p1/2 spin-orbit components with binding energies of 1020 and 1043 eV, respectively.

4. Conclusions

Electrospinning is an important technique for fabricating polymer and 1D metal oxide nanofibers. The desired characteristics can be measured by nanofibers' structure, which is controlled by various parameters including electrospinning solution, process, and ambient parameters. Selected polymers are critically used to prepare electrospun fibers' templates for this approach. The polymers used in this approach can be categorized into three classes including natural, synthetic, and copolymers. Electrospinning technique represents a vital promise with some borders for many applications such as small pore size and lack of cellular infiltration, which can be enhanced through multilayering and using of polymers of altered degradation grades. The technique has been adapted to produce many 1D metal oxide nanostructures for different important applications. This chapter introduced the fabrication of various metal oxide nanofibers which has attracted a significant attention because of their vital applications in the recent years such as tin oxide, zinc oxide, titanium oxide, and nickel oxide. Specific polymers were chosen as a sacrificial template to synthesize metal oxide nanofibers. After the annealing process, the organic specimens will be decomposed and the metal oxide nanofibers will be produced. Scanning electron microscope, X-ray diffraction, and X-ray photoelectron spectroscopy are used to characterize electrospun metal oxide nanofibers. The obtained data confirm the formation of homogeneously distributed metal oxide nanofibers.

Author details

Moustafa M. Zagho[1,2] and Ahmed Elzatahry[2*]

*Address all correspondence to: aelzatahry@qu.edu.qa

1 Center for Advanced Materials (CAM), Qatar University, Doha, Qatar

2 College of Arts and Science, Qatar University, Doha, Qatar

References

[1] Reneker DH, Yarin AL, Fong H, Koombhongse S. Bending instability of electrically charged liquid jets of polymer solutions in electrospinning. J Appl Phys. 2000;87:4531–4547.

[2] Schreuder-Gibson HL, Gibson P, Senecal K, Sennett M, Walker J, Yeomans W. Protective textile materials based on electrospun nanofibers. J Adv Mater. 2002;34:44–55.

[3] Huang ZM, Zhang YZ, Kotaki M, Ramakrishna S. A review on polymer nanofibers by electrospinning and their applications in nanocomposites. Compos Sci Technol. 2003;63:2223–2253.

[4] Theron SA, Yarin AL, Zussman E, Kroll E. Multiple jets in electrospinning: experiment and modeling. Polymer. 2005;46:2889–2899.

[5] Ma Z, Kotaki M, Inai R, Ramakrishna S. Potential of nanofiber matrix as tissue engineering scaffolds. Tissue Eng. 2005;11:101–109.

[6] Ahn YC, Park SK, Kim GT, Hwang YJ, Lee CG, Shin HS. Development of high efficiency nanofilters made of nanofibers. Curr Appl Phys. 2006;6:1030–1035.

[7] Lannutti J, Reneker D, Ma T, Tomasko D, Farson D. Electrospinning for tissue engineering scaffolds. Mater Sci Eng C. 2007;27:504–509.

[8] Hunley MT, Long TE. Electrospinning functional nanoscalefibers: a perspective for the future. Polym Int. 2008;57:385–389.

[9] Reneker DH, Yarin AL. Electrospinning jets and polymer nanofibers. Polymer. 2008;49:2387–2425.

[10] Zussman E, Theron A, Yarin AL. Formation of nanofiber crossbars in electrospinning. Appl Phys Lett. 2003;82:973–975.

[11] He J, Wan YQ, Yu JY. Scaling law in electrospinning: relationship between electric current and solution flow rate. Polymer. 2005;46:2799–2801.

[12] Luu YK, Kim K, Hsiao BS, Chu B, Hadjiargyrou M. Development of a nanostructured DNA delivery scaffold via electrospinning of PLGA and PLA-PEG block copolymers. J Control Release. 2003;89:341–353.

[13] Subbiah T, Bhat GS, Tock RW, Parameswaran S, Ramkumar SS. Electrospinning of nanofibers. J Appl Polym Sci. 2005;96:557–569.

[14] Ramakrishna S, Fujihara K, Teo WE, Yong T, Ma Z, Ramaseshan R. Electrospun nanofibers: solving global issues. Mater Today. 2006;9:40–50.

[15] Cui W, Zhou S, Li X, Weng J. Drug-loaded biodegradable polymeric nanofibers prepared by electrospinning. Tissue Eng. 2006;12:1070–1070.

[16] Wu Y, He JH, Xu L, Yu JY. Electrospinning drug-loaded poly (butylenes succinate-cobytylene terephthalate) (PBST) with acetylsalicylic acid (aspirin). Int J Electrospun Nanofibers Appl. 2007;1:1–6.

[17] Barnes CP, Sell SA, Knapp DC, Walpoth BH, Brand DD, Bowlin GL. Preliminary investigation of electrospun collagen and polydioxanone for vascular tissue engineering applications. Int J Electrospun Nanofibers Appl. 2007;1:73–87.

[18] Welle A, Kroger M, Doring M, Niederer K, Pindel E, Chronakis S. Electrospun aliphatic polycarbonates as tailored tissue scaffold materials. Biomaterials. 2007;28:2211–2219.

[19] Liang D, Hsiao BS, Chu B. Functional electrospun nanofibrous scaffolds for biomedical applications. Adv Drug Deliv Rev. 2007;59:1392–1412.

[20] Chong EJ, Phan TT, Lim IJ, Zhang YZ, Bay BH, Ramakrishna S. Evaluation of electrospun PCL/gelatinnanofibrous scaffold for wound healing and layered dermal reconstitution. Acta Mater. 2007;3:321–330.

[21] Ma ZW, Kotaki M, Ramakrishna S. Electrospun cellulose nanofiber as affinity membrane. J Membr Sci. 2005;265:115–123.

[22] Stankus JJ, Guan J, Wagner WR. Fabrication of biodegradable elastomeric scaffolds with sub-micron morphologies. J Biomed Mater Res. 2004;70A:603–614.

[23] Matthews JA, Wnek GE, Simpson DG, Bowlin GL. Electrospinning of collagen nanofibers. Biomacromolecules. 2002;3:232–238.

[24] Um IC, Fang DF, Hsiao BS, Okamoto A, Chu B. Electro-spinning and electro-blowing of hyaluronic acid. Biomacromolecules. 2004;5:1428–1436.

[25] Yarin AL, Zussman E. Upward needleless electrospinning of multiple nanofibers. Polymer. 2004;45:2977–2980.

[26] Tomaszewski W, Szadkowski M. Investigation of electrospinning with the use of a multi-jet electrospinning head. Fibres Text East Eur. 2005;13:22–26.

[27] Dosunmu OO, Chase GG, Kantaphinan W, Reneker DH. Electrospinning of polymer nanofibres from multiple jets on a porous tubular surface. Nanotechnology. 2006;17:1123–1127.

[28] Eichhorn SJ, Sampson WW. Statistical geometry of pores and statistics of porous nanofibrous assemblies. J R Soc Interface. 2005;2:309–318.

[29] Ekaputra AK, Prestwich GD, Cool SM, Hutmacher DW. Combining electrospun scaffolds with electrosprayed hydrogels leads to three-dimensional cellularization of hybrid constructs. Biomacromolecules. 2008;9:2097–2103.

[30] Cai SS, Liu YC, Shu XZ, Prestwich GD. Injectable glycosaminoglycan hydrogels for controlled release of human basic fibroblast growth factor. Biomaterials. 2005;26:6054–6067.

[31] Chew SY, Wen Y, Dzenis Y, Leong KW. The role of electrospinning in the emerging field of nanomedicine. Curr Pharm Des. 2006;12:4751-4770.

[32] Sill TJ, von Recum HA. Electrospinning: applications in drug delivery and tissue engineering. Biomaterials. 2008;29:1989–2006.

[33] Taylor GI. Electrically driven jets. Proc R Soc Lond A Math Phys Sci. 1969;313:453–475.

[34] Adomaviciute E, Rimvydas M. The influence of applied voltage on poly (vinyl alcohol) (PVA) nanofibre diameter. Fibers Text East Eur. 2007;15:64–65.

[35] Jiang HL, Fang DF, Hsiao BS, Chu B, Chen WL. Optimization and characterization of dextran membranes prepared by electrospinning. Biomacromolecules. 2004;5:326–333.

[36] Li M, Mondrinos MJ, Gandhi MR, Ko FK, Weiss AS, Lelkes PI. Electrospun protein fibers as matrices for tissue engineering. Biomaterials. 2005;26:5999–6008.

[37] Li J, He A, Zheng J, Han CC. Gelatin and gelatin-hyaluronic acid nanofibrous membranes produced by electrospinning of their aqueous solutions. Biomacromolecules. 2006;7:2243–2247.

[38] Li C, Vepari C, Jin HJ, Kim HJ, Kaplan DL. Electrospun silk-BMP-2 scaffolds for bone tissue engineering. Biomaterials. 2006;27:3115–3124.

[39] Zhang Y, Ouyang H, Lim CT, Ramakrishna S, Huang ZM. Electrospinning of gelatin fibers and gelatin/PCL composite fibrous scaffolds. J Biomed Mater Res B Appl Biomater. 2005;72:156–165.

[40] Zhang YZ, Venugopal J, Huang ZM, Lim CT, Ramakrishna S. Crosslinking of the electrospun gelatin nanofibers. Polymer. 2006;47:2911–2917.

[41] Zhong S, Teo WE, Zhu X, Beuerman RW, Ramakrishna S, Yung LYL. An aligned nanofibrous collagen scaffold by electrospinning and its effects on in vitro fibroblast culture. J Biomed Mater Res A. 2006;79A:456–463.

[42] Zeugolis DI, Khew ST, Yew ESY, Ekaputra AK, Tong YW, Yung LYL. Electro-spinning of pure collagen nano-fibres—just an expensive way to make gelatin? Biomaterials. 2008;29:2293–2305.

[43] Kwon IK, Matsuda T. Co-electrospun nanofiber fabrics of poly (L-lactide-co-ε-caprolactone) with type I collagen or heparin. Biomacromolecules. 2005;6:2096–2105.

[44] Yang L, Fitie CFC, Werf KOV, Bennink ML, Dijkstra PJ, Feijen J. Mechanical properties of single electrospun collagen type I fibers. Biomaterials. 2008;29:955–962.

[45] Neal RA, McClugage III SG, Link MC, Sefcik LS, Ogle RC, Botchwey EA. Laminin nanofiber meshes that mimic morphological properties and bioactivity of basement membranes. Tissue Eng Part C. 2008;15:11–21.

[46] Hakkarainen M. Aliphatic polyesters: abiotic and biotic degradation and degradation products. Adv Polym Sci. 2002;157:113–138.

[47] Jing Z, Xu XY, Chen XS, Liang QZ, Bian XC, Yang LX. Biodegradable electrospun fibers for drug delivery. J Control Release. 2003;92:227–231.

[48] Boland ED, Wnek GE, Simpson DG, Pawlowski KJ, Bowlin GL. Tailoring tissue engineering scaffolds using electrostatic processing techniques: a study of poly (glycolic acid) electrospinning. J Macromol Sci Pure Appl Chem A. 2001;38:1231–1243.

[49] Kenawy ER, Bowlin GL, Mansfield K, Layman J, Simpson DG, Sanders EH. Release of tetracycline hydrochloride from electrospun poly (ethylene-co-vinylacetate, poly (lactic acid), and a blend. J Control Release. 2002;81:57–64.

[50] Ho BC, Lee YD, Chin WK. Thermal degradation of polymethacrylic acid. J Polym Sci Polym Chem. 1992;30:2389–2397.

[51] Bhattarai N, Cha DI, Bhattarai SR, Khil MS, Kim HY. Biodegradable electrospun mat: novel block copolymer of poly (p-dioxanone-co-lactide)-block-poly (ethylene glycol). J Polym Sci B Polym Phys. 2003;41:1955–1964.

[52] Dharmaraj N, Kim CH, Kim KW, Kim HY, Suh EK. Spectral studies of SnO_2 nanofibers prepared by electrospinning method. Spectrochim Acta A. 2006;64:136–140.

[53] Guan H, Shao C, Chen B, Gong J, Yang X. A novel method for making CuO superfine fibers via an electrospinning technique. Inorg Chem Commun. 2003;6:1409–1411.

[54] Macias M, Chacko A, Ferraris JP, Balkus KJ. Electrospunmesoporous metal oxide fibers. Micropor Mesopor Mater. 2005;86:1–13.

[55] Yang XH, Shao CL, Guan HY, Li XL, Gong J. Preparation and characterization of ZnO nanofibers by using electrospun PVA/zinc acetate composite fiber as precursor. Inorg Chem Commun. 2004;7:176–178.

[56] Onozuka K, Ding B, Tsuge Y, Naka T, Yamazaki M, Sugi S, Ohno S, Yoshikawa M, Shiratori S. Electrospinning processed nanofibrous TiO_2 membranes for photovoltaic applications. Nanotechnology. 2006;17:1026–1031.

[57] Yang XH, Shao CL, Liu YC, Mu RX, Guan HY. Nanofibers of CeO_2 via an electrospinning technique. Thin Solid Films. 2005;478:228–231.

[58] Wang D, Chu XF, Gong ML. Gas-sensing properties of sensors based on single-crystalline SnO_2 nanorods prepared by a simple molten-salt method. Sens Actuators B Chem. 2006;117:183–187.

[59] Yang MR, Chu SY, Chang RC. Synthesis and study of the SnO_2 nanowires growth. Sens Actuators B Chem. 2007;122:269–273.

[60] Luo SH, Fan JY, Liu WL, Zhang M, Song ZT, Lin CL, Wu XL, Chu PK. Synthesis and low-temperature photoluminescence properties of SnO_2 nanowires and nanobelts. Nanotechnology. 2006;17:1695–1699.

[61] Comini E, Faglia G, Sberveglieri G, Calestani D, Zanotti L, Zha M. Tin oxide nanobelts electrical and sensing properties. Sens Actuators B Chem. 2005;111:2–6.

[62] Hu JQ, Bando Y, Golberg D. Self-catalyst growth and optical properties of novel SnO_2 fishbone-like nanoribbons. Chem Phys Lett. 2003;372:758–762.

[63] Ding B, Wang M, Yu J, Sun G. Gas sensors based on electrospun nanofibers. Sensors. 2009;9:1609–1624.

[64] Ding B, Kim J, Miyazaki Y, Shiratori S. Electrospun nanofibrous membrane coated quartz crystal microbalance as gas sensor for NH_3 detection. Sens Actuators B Chem. 2004;101:373–380.

[65] Liu HQ, Kameoka J, Czaplewski DA, Craighead HG. Polymeric nanowire chemical sensor. Nano Lett. 2004;4:671–675.

[66] Kessick R, Tepper G. Electrospun polymer composite fiber arrays for the detection and identification of volatile organic compounds. Sens Actuators B Chem. 2006;117:205–210.

[67] Luoh R, Hahn HT. Electrospun nanocomposite fiber mats as gas sensors. Compos Sci Technol. 2006;66:2436–2441.

[68] Kim ID, Rothschild A, Lee BH, Kim DY, Jo SM, Tuller HL. Ultrasensitive chemiresistors based on electrospun TiO_2 nanofibers. Nano Lett. 2006;6:2009–2013.

[69] Zhang Y, He XL, Li JP, Miao ZJ, Huang F. Fabrication and ethanol-sensing properties of micro gas sensor based on electrospun SnO_2 nanofibers. Sens Actuators B Chem. 2008;132:67–73.

[70] Wang G, Ji Y, Huang XR, Yang XQ, Gouma PI, Dudley M. Fabrication and characterization of polycrystalline WO_3 nanofibers and their application for ammonia sensing. J Phys Chem B. 2006;110:23777–23782.

[71] Khorami HA, Keyanpour-Rad M, Vaezi MR. Synthesis of SnO_2/ZnO composite nanofibers by electrospinning method and study of its ethanol sensing properties. Appl Surf Sci. 2011;257:7988–7992.

[72] Zhao Y, He X, Li J, Cao X, Jia J. Porous CuO/SnO_2 composite nanofibers fabricated by electrospinning and their H_2S sensing properties. Sens Actuators B Chem. 2012;165:82–87.

[73] Park JY, Asokan K, Choi SW, Kim S. Growth kinetics of nanograins in SnO_2 fibers and size dependent sensing properties. Sens Actuators B Chem. 2011;152:254–260.

[74] Zhang Y, Li J, An G, He X. Highly porous SnO_2 fibers by electrospinning and oxygen plasma etching and its ethanol-sensing properties. Sens Actuators B Chem. 2010;144:43–48.

[75] Santos JP, Fernández MJ, Fontecha JL, Matatagui D, Sayago I, Horrillo MC, Gracia I. Nanocrystalline tin oxide nanofibers deposited by a novel focused electrospinning

method. Application to the detection of TATP precursors. Sensors. 2014;14:24231–24243.

[76] Cheng L, Ma SY, Wang TT, Li XB, Luo J, Li WQ, Mao YZ, GZ DJ. Synthesis and characterization of SnO_2 hollow nanofibers by electrospinning for ethanol sensing properties. Mater Lett. 2014;131:23–26.

[77] Choi JK, Hwang IS, Kim SJ, Park JS, Park SS, Jeong U, Kang YC, Lee JH. Design of selective gas sensors using electrospun Pd-doped SnO_2 hollow nanofibers. Sens Actuators B. 2010;150:191–199.

[78] Li WQ, Ma SY, Li YF, Li XB, Wang CY, Yang XH, Cheng L, Mao YZ, Luo J, Gengzang DJ, Wan GX, Xu XL. Preparation of Pr-doped SnO_2 hollow nanofibers by electrospinning method and their gas sensing properties. J Alloys Compd. 2014;605:80–88.

[79] Du H, Wang J, Su M, Yao P, Zheng Y, Yu N. Formaldehyde gas sensor based on SnO_2/In_2O_3 hetero-nanofibers by a modified double jets electrospinning process. Sens Actuators B. 2012;166:746–752.

[80] Tang W, Wang J, Yao P, Li X. Hollow hierarchical SnO_2-ZnO composite nanofibers with heterostructure based on electrospinning method for detecting methanol. Sens Actuators B. 2014;192:543–549.

[81] Hiroyuki U. Influence of surfactant micelles on morphology and photoluminescence of zinc oxide nanorods prepared by one-step chemical synthesis in aqueous solution. J Phys Chem C. 2007;111:9060–9065.

[82] Kind H, Yan HQ, Messer B, Law M, Yang PD. Nanowire ultraviolet photodetectors and optical switches. Adv Mater. 2002;14:158–160.

[83] Izaki M, Watase S, Takahashi H. Room-temperature ultraviolet light-emitting zinc oxide micropatterns prepared by low-temperature electrodeposition and photoresist. App Phys Lett. 2003;83:4930–4932.

[84] Hingorani S, Pillai V, Kumar P, Multani MS, Shah DO. Microemulsion mediated synthesis of zinc-oxide nanoparticles for varistor studies. Mater Res Bull. 1993;28:1303–1310.

[85] Sakohara S, Ishida M, Anderson MA. Visible luminescence and surface properties of nanosized ZnO colloids. J Phys Chem B. 1998;102:10169–10175.

[86] Zhang Z, Liu S, Chow S, Han MY. Modulation of the morphology of ZnO nanostructures via aminolytic reaction: from nanorods to nanosquamas. Langmuir. 2006;22:6335–6340.

[87] Ochanda F, Cho K, Andala D, Keane TC, Atkinson A, Jones WE. Synthesis and optical properties of co-doped ZnO submicrometer tubes from electrospun fiber templates. Langmuir. 2009;25:7547–7552.

[88] Huang MH, Feick H, Weber E, Wu Y, Tran N, Yang P. Catalytic growth of zinc oxide nanowires by vapor transport. Adv Mater. 2001;13:113–116.

[89] Kong XY, Wang ZL. Polar-surface dominated ZnO nanobelts and the electrostatic energy induced nanohelixes, nanosprings and nanospirals. Appl Phys Lett. 2004;84:975–978.

[90] Hughes WL, Wang ZL. Formation of piezoelectric single-crystal nanorings and nanobows. J Am Chem Soc. 2004;126:6703–6709.

[91] Wang ZL, Kong XY, Zuo JM. Induced growth of asymmetric nanocantilever arrays on polar surfaces. Phys Rev Lett. 2003;91:185502–185505.

[92] Ding B, Ogawa T, Kim J, Fujimoto K, Shiratori S. Fabrication of a superhydrophobic nanofibrous zinc oxide film surface by electrospinning. Thin Solid Films. 2008;516:2495–2501.

[93] Barakat NAM, Abadir MF, Sheikh FA, Kanjwal MA, Park SJ, Kim HY. Polymeric nanofibers containing solid nanoparticles prepared by electrospinning and their applications. Chem Eng J. 2010;156:487–495.

[94] Zhang Z, Li X, Wang C, Wei L, Liu Y, Shao C. ZnO hollow nanofibers: fabrication from facile single capillary electrospinning and applications in gas sensors. J Phys Chem C. 2009;113:19397–19403.

[95] Kanjwal MA, Sheikh FA, Barakat NAM, Li X, Kim HY, Chronakis IS. Zinc oxide's hierarchical nanostructure and its photocatalytic properties. Appl Surf Sci. 2012;258:3695–3702.

[96] Mauro AD, Zimbone M, Fragalà ME, Impellizzeri G. Synthesis of ZnO nanofibers by the electrospinning process. Mater Sci Semicond Process. 2016;42:98–101.

[97] Li W, Ma S, Yang G, Mao Y, Luo J, Cheng L, Gengzang D, Xu X, Yan S. Preparation, characterization and gas sensing properties of pure and Ce doped ZnO hollow nanofibers. Mater Lett. 2015;138:188–191.

[98] Park M, Han SM. Enhancement in conductivity through Ga, Al dual doping of ZnO nanofibers. Thin Solid Films. 2015;590:307–310.

[99] Wu MS, Wang MJ, Jow JJ, Yang WD, Hsieh CY, Tsai HM. Electrochemical fabrication of anatase TiO_2 nanostructure as an anode material for aqueous lithium-ion batteries. J Power Sources. 2008;185:1420–1424.

[100] Bojinov V, Grabchevb I. Synthesis and properties of new adducts of 2,2,6,6-tetramethylpiperidine and 2-hydroxyphenylbenzotriazole as polymer photostabilizers. J Photochem Photobiol A Chem. 2002;150:223–231.

[101] Manickam M, Singh P, Issa TB, Thurgate S. Electrochemical behavior of anatase TiO_2 in aqueous lithium hydroxide electrolyte. J Appl Electrochem. 2006;36:599–602.

[102] Reiman KH, Brace KM, Smith TJG, Nandhakumar I, Attard GS, Owen JR. Lithium insertion into TiO_2 from aqueous solution—facilitated by nanostructure. Electrochem Commun. 2006;8:517–522.

[103] He X, Yang CP, Zhang GL, Shi DW, Huang QA, Xiao HB, Liu Y, Xiong R. Supercapacitor of TiO_2 nanofibers by electrospinning and KOH treatment. J Mater Des. 2016;106:74–80.

[104] Ma S, Jia J, Tian Y, Cao L, Shi S, Li X, Wang X. Improved H_2S sensing properties of Ag/TiO_2 nanofibers. Ceram Int. 2016;42:2041–2044.

[105] Hao Y, Shao X, Li B, Hu L, Wang T. Mesoporous TiO_2 nanofibers with controllable Au loadings for catalytic reduction of 4-nitrophenol. Mater Sci Semicond Process. 2015;40:621–663.

[106] Tolba GMK, Barakat NAM, Bastaweesy AM, Ashour EA, Abdelmoez W, El-Newehy MH, Al-Deyab SS, Kim HY. Hierarchical TiO_2/ZnO nanostructure as novel non-precious electrocatalyst for ethanol electrooxidation. J Mater Sci Technol. 2015;31:97–105.

[107] Li L, Cheng B, Wang Y, Yu J. Enhanced photocatalytic H_2-production activity of bicomponent NiO/TiO_2 composite nanofibers. J Colloid Interface Sci. 2015;449:115–121.

[108] Mohamed IMA, Dao VD, Barakat NAM, Yasin AS, Yousef A, Choi HS. Efficiency enhancement of dye-sensitized solar cells by use of ZrO_2-doped TiO_2 nanofibers photoanode. J Colloid Interface Sci. 2016;476:9–19.

[109] Liu M, Wang Y, Li P, Cheng Z, Zhang Y, Zhang M, Hu M, Li J. Preparation and characterization of multilayer NiOnano-products via electrospinning. Appl Surf Sci. 2013;284:453–458.

[110] Qu Y, Zhou W, Miao X, Li Y, Jiang L, Pan K, Tian G, Ren Z, Wang G, Fu H. A new layered photocathode with porous NiO nanosheets: an effective candidate for p-type dye-sensitized solar cells. Chemistry. 2013;8:3085–3090.

[111] Sialvi MZ, Mortimer RJ, Wilcox GD, Teridi AM, Varley TS, Wijayantha KGU, Kirk CA. Electrochromic and colorimetric properties of Nickel(II) oxide thin films prepared by aerosol-assisted chemical vapor deposition. ACS Appl Mater Interfaces. 2013;5:5675–5682.

[112] Macdonald TJ, Xu J, Elmas S, Mange YJ, Skinner WM, Xu H, Nann T. NiO nanofibers as a candidate for a nanophotocathode. Nanomaterials. 2014;4:256–266.

[113] Jian J, Luo F, Gao C, Suo C, Wang X, Song H, Hu X. Synthesis of La-doped NiO nanofibers and their electrochemical properties as electrode for supercapacitors. Ceram Int. 2014;40:6973–6977.

[114] Elzatahry A. Polyacrylonitrile electrospun nanofiber as a template to prepare NiO nanostructure electrocatalyst. Int J Electrochem Sci. 2014;9:22–31.

[115] Choi JM, Byun JH, Kim SS. Influence of grain size on gas-sensing properties of chemiresistive p-type NiO nanofibers. Sens Actuators B. 2016;227:149–156.

[116] Luo X, Zhang Z, Wan Q, Wu K, Yang N. Lithium-doped NiO nanofibers for nonenzymatic glucose sensing. Electrochem Commun. 2015;61:89–92.

[117] Pascariu P, Airinei A, Olaru N, Petrila I, Nica V, Sacarescu L, Tudorache F. Microstructure, electrical and humidity sensor properties of electrospun NiO-SnO_2 nanofibers. Sens Actuators B. 2016;222:1024–1031.